THE JOURNAL OF BIOLOGICAL CHEMISTRY VOL. 290, NO. 46, pp. 27880–27889, November 13, 2015

Mechanisms of Ricin Toxin Neutralization Revealed through Engineered Homodimeric and Heterodimeric Camelid Antibodies*[S]

Received for publication, April 10, 2015, and in revised form, September 8, 2015 Published, JBC Papers in Press, September 22, 2015, DOI 10.1074/jbc.M115.658070

Cristina Herrera[‡§1], **Jacqueline M. Tremblay**[¶], **Charles B. Shoemaker**[¶], **and Nicholas J. Mantis**[‡§2]

From the [‡]*Division of Infectious Disease, Wadsworth Center, New York State Department of Health, Albany, New York 12208, the* [§]*Department of Biomedical Sciences, University at Albany School of Public Health, Albany, New York 12201, and the* [¶]*Department of Infectious Disease and Global Health, Tufts Cummings School of Veterinary Medicine, North Grafton, Massachuetts 01536*

Background: Bispecific heterodimeric camelid heavy chain-only antibodies (VHHs) have been shown to neutralize ricin toxin *in vivo*.
Results: Heterodimeric VHHs promote ricin aggregation in solution and block toxin attachment to cell surfaces.
Conclusion: The bispecific nature of the heterodimeric VHHs may be important for toxin neutralization *in vivo*.
Significance: Understanding mechanisms of toxin neutralization will lead to the development of new antitoxin agents.

Novel antibody constructs consisting of two or more different camelid heavy-chain only antibodies (VHHs) joined via peptide linkers have proven to have potent toxin-neutralizing activity *in vivo* against Shiga, botulinum, *Clostridium difficile*, anthrax, and ricin toxins. However, the mechanisms by which these so-called bispecific VHH heterodimers promote toxin neutralization remain poorly understood. In the current study we produced a new collection of ricin-specific VHH heterodimers, as well as VHH homodimers, and characterized them for their ability neutralize ricin *in vitro* and *in vivo*. We demonstrate that the VHH heterodimers, but not homodimers were able to completely protect mice against ricin challenge, even though the two classes of antibodies (heterodimers and homodimers) had virtually identical affinities for ricin holotoxin and similar IC_{50} values in a Vero cell cytotoxicity assay. The VHH heterodimers did differ from the homodimers in their ability to promote toxin aggregation in solution, as revealed through analytical ultracentrifugation. Moreover, the VHH heterodimers that were most effective at promoting ricin aggregation in solution were also the most effective at blocking ricin attachment to cell surfaces. Collectively, these data suggest that heterodimeric VHH-based neutralizing agents may function through the formation of antibody-toxin complexes that are impaired in their ability to access host cell receptors.

There remains a large demand in the public health community and military sectors for the development of prophylactics and therapeutics capable of neutralizing fast-acting plant and microbial toxins, especially those like botulinum neurotoxins, anthrax, and ricin toxin that have the potential to be used as biothreat agents (1–4). Although a number of promising toxin-neutralizing murine and humanized monoclonal antibodies (mAbs) are in the pipeline, the emergence of technologies surrounding the generation and expression of toxin-specific camelid heavy chain-only VH domains (VHHs)[3] has opened up new avenues for the rational design and delivery of antitoxin agents (5). VHHs with toxin-neutralizing activity have been described against botulinum neurotoxin (6), *Clostridium difficile* toxins TcdA and TcdB (7–9), Shiga toxins (10), ricin (11, 12), and anthrax toxin (13). X-ray crystallography of toxin-VHH complexes has provided novel insights into the mechanisms of toxin neutralization (7, 14) and single chain antibodies have been successfully delivered into the intracellular compartment of mammalian cells where they can effectively inactivate their targets (15).

We recently developed so-called VHH-based neutralizing agents (VNAs) consisting of two or more different VHHs covalently linked to each other via peptide spacers and expressed as single fusion proteins in *Escherichia coli* (6, 9–13). In general, the linked VHHs lead to enhanced *in vitro* and *in vivo* neutralization properties compared with the VHH monomers. This is especially true in the case of ricin toxin. For example, we produced and characterized five VHHs against the ricin enzymatic subunit (RTA) and one against the ricin binding subunit (RTB), each with potent toxin-neutralizing activity *in vitro* (12). The five RTA- and one RTB-specific VHHs were each able to neutralize ricin toxin *in vitro*, albeit with varying IC_{50} values. However, the monomeric VHHs were unable to neutralize ricin *in vivo*; when passively administered to mice, the monomeric VHHs, alone or in combination with other VHHs did not protect animals from ricin intoxication, although in some cases they extended time to death (11, 12). This was true even when

* This work was supported, in whole or in part, by National Institutes of Health Grant R03 AI097688 and Contract numbers HHSN272201400021C (to N. M. J.) and U54-AI057159 (to C. B. S.) from the NIAID. The content of this manuscript is solely the responsibility of the authors and does not necessarily represent the official views of NIAID or National Institutes of Health.
[1] Supported by a Carson Carr Diversity Scholarship from the University at Albany.
[S] This article contains supplemental Figs. S1 and S2.
[2] To whom correspondence should be addressed: Division of Infectious Disease, Wadsworth Center, 120 New Scotland Ave., Albany, NY 12208. Tel.: 518-473-7487; Fax: 518-402-4773; E-mail: nicholas.mantis@health.ny.gov.

[3] The abbreviations used are: VHH, heavy-chain VH domain; VNA, VHH-based neutralizing agent; RTA, ricin toxin A enzymatic subunit; RTB, ricin toxin B binding subunit; AUC, analytical ultracentrifugation; SPR, surface plasmon resonance.

VHH monomers were administered at 100:1 VHH:toxin stoichiometric ratios. On the other hand, heterodimer VNAs consisting of an anti-RTB VHH (RTB-B7) linked to one of three different RTA-specific VHHs (RTA-D10, RTA-E5, and RTA-F5) were each able to neutralize ricin *in vivo* at VHH:toxin stoichiometric ratios as low as 4:1, thereby making them as effective as the most potent murine mAbs described to date (16). It was not determined whether the bivalent and/or the bispecific nature of VNAs was critical in modulating toxin neutralizing activity in the mouse model.

Ricin provides a model system to begin to assess mechanisms by which VNAs but not VHH monomers promote toxin neutralization *in vivo*. Ricin is the prototypic member of the medically important superfamily A-B plant and bacterial toxins (17). RTA is an RNA *N*-glycosidase that inactivates eukaryotic ribosomes by catalyzing the hydrolysis of a universally conserved residue within the so-called sarcin/ricin loop of 28S rRNA (18, 19). RTB is a galactose- and *N*-acetylgalactosamine (Gal/GalNAc)-specific lectin that promotes ricin uptake into mammalian cells, including epithelial cells, sinusoidal endothelial cells, and macrophages (20, 21). RTB also mediates the retrograde transport of ricin from the plasma membrane to the trans-Golgi network and endoplasmic reticulum (ER), where RTA is liberated from RTB and retro-translocated into the cell cytoplasm (22, 23).

In the current study we engineered and characterized a new collection of ricin-specific VHH heterodimers and VHH homodimers. The VHH homodimers had *in vitro* toxin-neutralizing activities that were equivalent to or in some cases exceeded those of the VHH heterodimers. However, none of the VHH homodimers were able to protect mice against ricin intoxication. On the other hand, two of the three new VHH heterodimers, JNA10 and JNA11, were able to completely neutralize ricin *in vivo*. The same two VHH heterodimers promoted the formation of ricin toxin aggregates in solution and were highly effective at blocking toxin attachment to cell surfaces. We propose that heterodimeric VNAs may neutralize ricin *in vivo* through the formation of antibody-toxin complexes and thereby impair the ability of ricin to access host cell surfaces.

Experimental Procedures

Chemicals, Biological Reagents, and Cell Lines—Ricin toxin (*Ricinus communis* agglutinin II), FITC (fluorescein isothiocyanate)-labeled ricin, ricin toxin A (RTA) and B (RTB) subunits were purchased from Vector Laboratories (Burlingame, CA). Ricin was dialyzed against PBS at 4 °C in 10,000 molecular weight cutoff Slide-A-Lyzer dialysis cassettes (Pierce) prior to use in cytotoxicity and animal studies. D-(+)-Lactose was obtained from J. T. Baker (Center Valley, PA) and Sigma. Goat serum was purchased from Gibco. Anti-E-tag HRP-conjugated mAb was purchased from Bethyl Laboratories, Inc. (Montgomery, TX). Unless noted otherwise, all other chemicals were obtained from Sigma. Cell lines and cell culture media were obtained from the tissue culture media core facility at the Wadsworth Center. THP-1 cells were grown in RPMI with 10% FBS; Vero cells were grown in DMEM with 10% FBS. All cell lines were maintained in 37 °C with 5% CO_2 incubators, unless noted otherwise.

Mouse Strains, Animal Care, and Immunizations—Mouse experiments were performed as described (12). Female BALB/c or Swiss Webster mice ~8–10 weeks of age were purchased from Taconic Labs (Hudson, NY). Animals were housed under conventional, specific pathogen-free conditions and were treated in compliance with the Wadsworth Center's Institutional Animal Care and Use Committee (IACUC) guidelines. For challenge experiments, groups of mice ($n = 5$ per group) were injected by intraperitoneally with a mixture of ricin toxin (RT; 2 μg) and corresponding VHH (12 μg) or IgG mAb PB10 (12 μg) in 0.4 ml of PBS. For pre- and post-exposure experiments, mice were injected intraperitoneally with antibody 2 h prior or post-ricin challenge. Mice received antibody premixed with ricin at time 0. The onset of hypoglycemia as a measure of toxin-induced morbidity was measured using a hand-held glucometer on days 0, 2, and 5 (Accu-Chek Advantage, Roche, Indianapolis, IN). Mice were euthanized by carbon dioxide (CO_2) asphyxiation when they became overtly moribund and/or blood glucose levels fell below 25 mg/dl. Survival was monitored for up to 8 days. At no point in the study were the animals administered analgesics or anesthetics so as not to confound the effects of antibody treatments.

VHH and VNA Expression and Purification—Monomer, homodimer, and heterodimer camelid antibodies were produced in *E. coli* Rosetta-gami (Novagen, Madison, WI) as thioredoxin fusion proteins, following in-frame insertion of their coding DNAs into the pET32 expression vector (Novagen). Purification was achieved using a nickel affinity column (Invitrogen, ThermoFisher Scientific, Grand Island, NY) to the vector-encoded hexahistidine and detection employed anti-E-tag recognition of the carboxyl-terminal E-tag epitope. Coding DNAs were engineered or synthesized for insertion into the vector, and all dimers contain a $(GGGGS)_3$ flexible spacer (24). Purity and concentrations of the antibody preparations was determined by SDS-PAGE with comparisons to internal standards.

Determining VHH Specificity Using Competition ELISAs—Competition ELISAs were performed as described previously (11). In brief, Nunc Immuno MicroWell 96-well plates from ThermoFisher Scientific (Rochester, NY) were coated overnight with 0.1 μg/well of ricin (15 nM) in PBS (pH 7.4). The following day the plates were blocked with 2% goat serum in PBS (pH 7.4) for 2 h. Then, VHHs (3.3 nM) at constant concentrations were mixed with 2-fold dilutions of RTA, RTB, or ricin (starting at 200 μg/ml) and incubated for 30 min, then applied to ELISA plates coated with ricin or BSA (0.1 μg/well; 8 nM) as a control for 1 h. Plates were developed with HRP anti-E-tag (1:10,000) and TMB (KPL, Gaithersburg, MD). The reactions were stopped with 1 M phosphoric acid and absorbance was read at 450 nm using the VersaMax Microplate Reader with Softmax Pro 5.2 software (Molecular Devices, Sunnyvale, CA). All samples were performed at least in triplicate.

Ricin Binding Assays Using THP-1 Cells and Flow Cytometry—Ricin binding to cell surfaces was performed as described (25). Briefly, THP-1 cells were collected by gentle, low speed centrifugation (5 min at 400 × *g*). The resulting cell

pellets were suspended to ~5 × 10^6 cells/ml and seeded (200 μl/well) into clear U-bottom 96-well plates (BD Bioscience, San Jose, CA). FITC-labeled ricin (50 nM) was mixed with VHHs (100 nM) or lactose (88 mM) and incubated for 30 min on ice in the dark prior to being added to THP-1 cells. Cells were incubated for 30 min on ice to prevent internalization, washed twice with PHEM buffer to remove unbound antibody-toxin complexes, and then fixed for 15 min with 4% paraformaldehyde in PHEM. FITC-labeled ricin binding to the surface of THP-1 cells was measured using the FACS Calibur flow cytometer (BD Bioscience). A minimum of 10,000 events was analyzed per sample; experiments were repeated three independent times.

Sedimentation Velocity Analytical Ultracentrifugation (AUC)—Ricin and VHHs were mixed at a 1:1 molar ratio and 2-fold dilutions were made, as previously described (11). Samples were mixed for at least 1 h before being subjected to AUC and all three dilution samples were run in parallel. Sedimentation velocity experiments were conducted in a Beckman Optima XL-I analytical ultracentrifuge (Beckman Coulter Inc., Brea, CA) at 20 °C at a rotor speed of 50,000 rpm. Double-sector charcoal-filled epon centerpieces were filled with a sample volume of 400 μl and the reference volume of dialysis buffer was 420 μl. Absorption measurements were made at 280, 230, or 225 nm, depending on the protein concentration. Samples were run in an An-60 Ti four-hole rotor with zero time between scans. Care was taken to have the rotor at thermal equilibrium for 1 h before accelerating directly to the speed of the experiment. The data were analyzed by the found in SEDFIT (26). The experimentally calculated sedimentation coefficients were converted to $s_{20,w}$ values within the SEDFIT software and graphed using Origins (OriginLab Corp., Northampton, MA).

Surface Plasmon Resonance (SPR) Kinetic Analysis—Kinetics (k_a, k_d) and equilibrium dissociation constants were determined as previously described by SPR using the ProteOn XPR36 (Bio-Rad Inc.) (14). A general layer compact (GLC) chip was equilibrated in running buffer PBS, 0.005% Tween (PBS-T, pH 7.4) at a flow rate of 30 μl/min for ricin immobilization. Following EDAC (200 mM), sulfo-NHS (50 mM) activation (3 min), ricin was diluted in 10 mM sodium acetate (pH 5.0) at two different concentrations (4 and 8 μg/ml) and immobilized (2 min). A third vertical channel received only acetate buffer and served as a reference channel. The surfaces were deactivated using 1 M ethanolamine (5 min). Ricin densities of 1099 and 2116 response units were obtained in the respective channels. The ProteOn MCM was then rotated to the horizontal orientation for antibody experiments. Binding of the antibodies was determined across five different concentrations ranging from 5 to 100 nM. Antibody solutions were made in PBS-T (pH 7.4). Antibody injections were made at 50 μl/min for 480 s and dissociation times varied from 1 to 6 h. The GLC chip was regenerated using two injections of 10 mM glycine (pH 1.5) each at 100 μl/min for 18 s. All experiments were performed at 25 °C. To calculate the kinetic constants, the data obtained were modeled using the Langmuir fit, selecting local settings for calculating response unit max and grouped settings for kinetics values, using the ProteOn Manager Software 3.1.0 (version 3.1.0.6) (Bio-Rad Inc.).

TABLE 1
Molecular weight for homodimers and heterodimers as determined by SECMALS

HD	Molecular mass
	Da
JJX21	42,190 ± 2.3%
JNA11	44,730 ± 2.4%
JNA10	50,750 ± 1.6%
JNA6	51,700 ± 2.7%
JNA8	48,250 ± 2.5%
JNA14	50,740 ± 2.0%
JNA2	48,870 ± 1.3%
JNA3	ND[a]

[a] ND, not determined; VHH JNA3 had insufficient signal for light scattering due to low concentration.

Size Exclusion Chromatography Coupled with Multiangle Light Scatter (SECMALS)—Antibody samples (200 μl), at a range of concentrations in PBS (pH 7.4), were passed through a 0.2-μm Whatman Anotop syringe filter (GE Healthcare Life Sciences) and then injected onto a Waters 300 SW column (8.0 × 300 mm), which accommodates a separation range of 10,000–300,000 M_r. The column was fully equilibrated and the system template routinely calibrated with BSA standards. The Varian HPLC is outfitted with an in-line 18 angle Wyatt Dawn Heleos laser light-scattering detector and a Wyatt Optilab rEX refractive index detector. Molecular masses were calculated from laser light scatter data using the ASTRA (version 6.1.2.84) software package from Wyatt Technology (Santa Barbara, CA). In all cases the measured M_r were in agreement with anticipated M_r (Table 1; supplemental Fig. S1).

Statistical Analyses and Software—Statistical analysis and graphs were carried out using GraphPad Prism 5 (GraphPad Software, San Diego, CA). For survival studies, statistical significance was determined using the Log-rank (Mantel-Cox) test. Analysis of variance was used to determine the statistical significance of ricin binding comparing the ricin control to each corresponding antibody treatment for the flow cytometry experiments.

Results

Engineering New Bispecific VHH Heterodimers Consisting of Neutralizing and Weakly Neutralizing Monomeric Constituents—We previously reported that three different VHH heterodimers (JJX12, JJX3, and JJX21), each consisting of potent toxin-neutralizing, RTA- and RTB-specific monomers, were able to protect mice from lethal dose ricin challenge when co-injected with toxin (11, 12). VHH heterodimers in the case of ricin consist of two different VHH monomers covalently linked to each other via a peptide spacer and expressed and purified from *E. coli* as a single fusion protein. The prophylactic and therapeutic potential of one of the heterodimers (JJX21) is shown in Fig. 1*A*; antibody treatment 2 h before or 2 h after ricin challenge was sufficient to fully protect mice from toxin-induced death. In this respect, JJX21 is similar to PB10 (Fig. 1*B*), one the most potent murine mAbs described to date (27).

To identify the attributes of VHH heterodimers associated with ricin toxin neutralization *in vivo*, we created three new heterodimers, JNA10, JNA11, and JNA8. JNA10 and JNA11 each consist of an RTA-specific and RTB-specific monomer

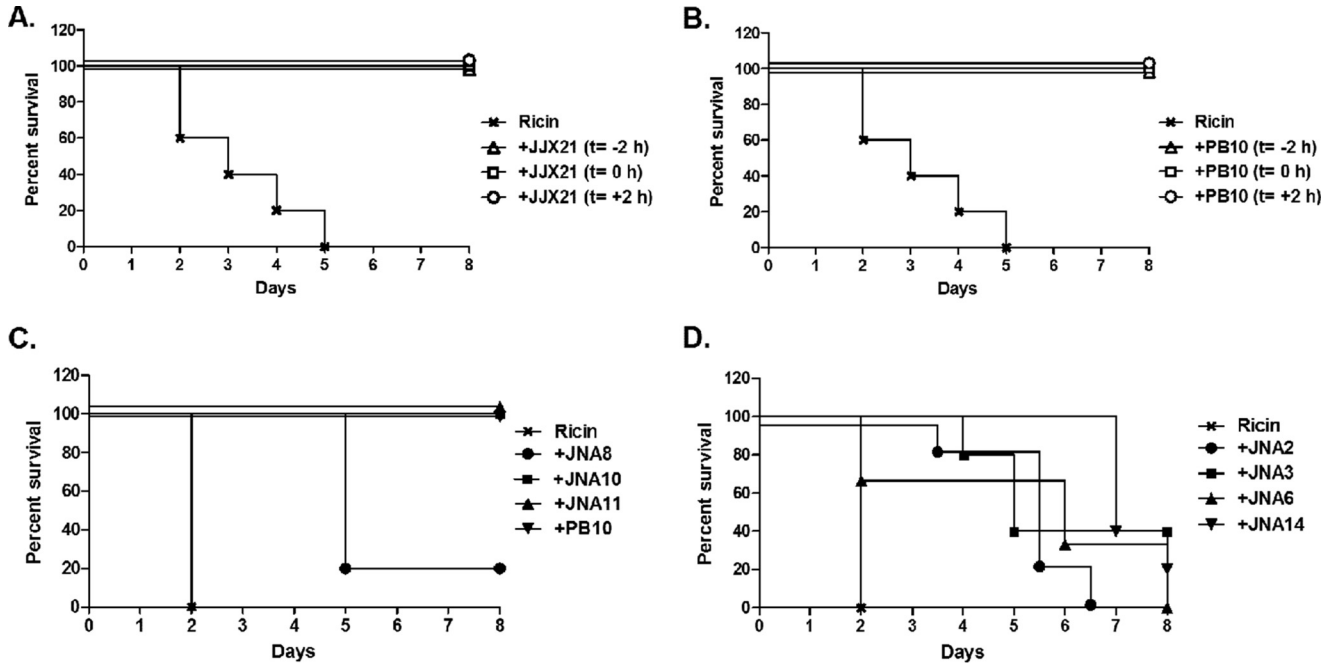

FIGURE 1. **Neutralization of ricin toxin by VHH heterodimers and homodimers in a mouse model.** *A,* VHH heterodimer JJX21, and *B,* mAb PB10 were each administered to adult BALB/c mice ($n = 5$ mice per group) 2 h prior ($t = -2$ h), concurrent with ($t = 0$), or 2 h after ($t = +2$ h) a 10× LD_{50} of ricin challenge. Survival was monitored for 8 days. *C,* VHH heterodimers (JNA8, JNA10, and JNA11), or *D,* VHH homodimers (JNA2, JNA3, JNA6, and JNA14) were mixed with 10× LD_{50} of ricin at an 8:1 molar VHH:toxin ratio, and then injected intraperitoneally into BALB/c mice ($n = 5$ mice per group). Survival was monitored for a total of 8 days. Antibody PB10 was used as a positive control for these studies, as described under "Experimental Procedures." *Panels A* and *B* correspond to a single experiment with shared controls, but were separated for clarity. It should be noted that VHH constructs JNA8, JNA2, JNA3, JNA6, and JNA14 significantly extend time to death, as compared with toxin-only treated mice ($p < 0.05$; Log-Rank Mantel-Cox test).

TABLE 2
Characteristics of VHH monomers

VHH[b]	K_D	EC_{50}[a]			
		IC_{50}[c]	Ricin	RTA	RTB
	M	nM		nM	
RTA-D10	1.1×10^{-10}	25	6.2	6.3	
RTA-E5	2.3×10^{-10}	5	3.1	3.1	
RTA-F5	2.8×10^{-10}	5	6.2	12.5	
RTA-F6	7.2×10^{-10}	>330	6.2	12.5	
RTB-B7	0.05×10^{-10}	1.5	6.2		88.2
RTB-D12	ND[d]	NA[e]	47.7		5.9

[a] Value indicates the effective concentration of VHHs required to achieve 50% maximal binding to ricin, RTA or RTB for competition ELISAs.
[b] Underlining indicates neutralizing VHHs.
[c] Values previously published indicating the concentration of VHHs required to neutralize 50% of ricin in a Vero cell assay (12).
[d] ND, not determined.
[e] NA, not applicable as there was no detectable neutralizing activity.

TABLE 3
Characteristics of VHH heterodimers and homodimers

HD[a]	VHH Pairings[b]		Protection[c]	IC_{50}[d]
				nM
JJX21	RTA-E5	RTB-B7	+	1*
JNA10	RTA-F6	RTB-B7	+	0.1
JNA11	RTA-E5	RTB-D12	+	0.1
JNA8	RTA-F6	RTB-D12	−	0.1
JNA6	RTB-B7	RTB-B7	−	0.5
JNA2	RTA-D10	RTA-D10	−	10
JNA3	RTA-E5	RTA-E5	−	1
JNA14	RTA-D10	RTA-E5	−	2

[a] HD, heterodimer or homodimer.
[b] Underlining indicates neutralizing VHHs.
[c] Plus (+) symbol indicates VHHs that passively protected mice against a 10 × LD_{50} ricin challenge and minus (−) symbol indicates VHHs that did not confer complete protection.
[d] Value indicates the concentration of VHHs required to neutralize 50% of ricin in a Vero cell cytotoxicity assay. (*) Indicates IC_{50} values previously published (12).
[e] Value indicates the effective concentration of VHHs required to achieve 50% maximal binding to ricin, RTA, or RTB for competition ELISAs.

in which one monomer has strong *in vitro* toxin-neutralizing activity and one monomer has weak or undetectable toxin-neutralizing activity (Tables 2 and 3). JNA8 consists of a weak toxin-neutralizing RTA-specific VHH monomer (RTA-F6) joined to a non-neutralizing RTB-specific monomer (RTB-B9).

The three new VHH heterodimers were examined with respect to their affinities for ricin holotoxin, *in vitro* toxin-neutralizing activities, and capacity to passively protect mice against ricin toxin challenge. Direct ELISAs confirmed that JNA10, JNA11, and JNA8 were bispecific and capable of binding to RTA and RTB (Fig. 2, *A*, *D*, and *G*). As further (indirect) evidence of their bispecificity, we found that attachment of JNA10, JNA11, and JNA8 to plate-bound ricin was inhibited by soluble ricin (Fig. 2, *B*, *E*, and *H*) but not soluble RTA or RTB (Fig. 2, *C*, *F*, and *I*). It should be noted that binding of JNA10 and JNA8 with plate-bound RTA was only modest because the VHH monomer common to both antibodies, RTA-F6, is proposed to recognize an epitope on RTA that is near the interface of RTB (12). However, Fig. 2 also demonstrates that RTA-F6 is fully functional because the binding of JNA10 and JNA8 to plate-bound ricin was unaffected when the antibodies' B-subunit-specific VHH components were saturated with soluble RTB. These data indicate RTA-F6 is sufficient to promote JNA10 and JNA8 binding to ricin.

By SPR it was determined that the dissociation constants (K_D) of JNA10, JNA11, and JNA8 for ricin were virtually identical to each other (2.70×10^{-12}, 1.67×10^{-12}, and 4.27×10^{-12} M, respectively) (Table 4). Moreover, in a Vero cell cytotoxicity assay, JNA10 and JNA11 each had IC_{50} values of 0.1 nM,

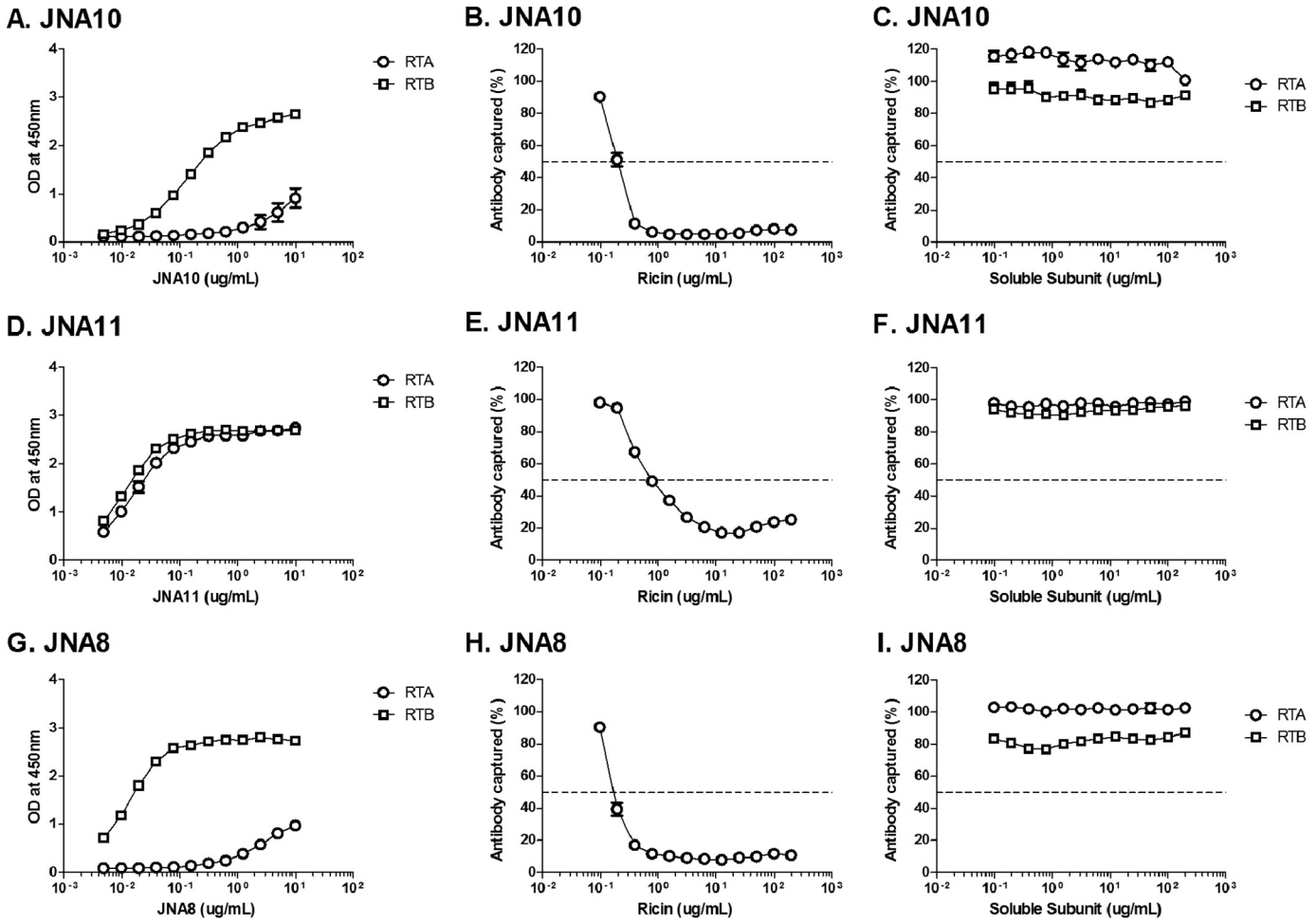

FIGURE 2. **Recognition of soluble ricin and ricin subunits by bispecific VHH heterodimers.** *Panels A*, *D*, and *G*, direct ELISAs in which microtiter plates were coated with RTA or RTB, as indicated, and then probed with 2-fold serial dilutions of JNA10 (*A*), JNA11 (*D*), or JNA8 (*G*). Optical density (*OD*) at 450 nm is shown on the *y* axis. *Panels B*, *C*, *E*, *F*, *H*, and *I*, competition ELISA in which microtiter plates were coated with ricin and then probed with VHH heterodimers (*B* and *C*) JNA10, JNA11 (*E* and *F*), or JNA8 (*H* and *I*) in the presence of 2-fold serial dilutions of soluble ricin (*middle panels*), RTA or RTB (*right panels*). The percent of antibody bound (captured) to the plate is indicated on the *y* axis. The results represent a single representative experiment done in triplicate with each point indicating mean ± S.D. In some instances *error bars* are masked by symbol and therefore not visible.

TABLE 4

Affinity and dissociation constants of VHH homodimers and heterodimers

VHH	k_a	k_d	K_D	K_D (calculated)[a]
	1/ms	*1/s*		*M*
JJX21	2.0×10^5	7.4×10^{-6}	3.84×10^{-11}	$<7.5 \times 10^{-11}$
JNA6	4.58×10^5	9.55×10^{-7}	2.10×10^{-12}	$<6.22 \times 10^{-12}$
JNA2	1.34×10^6	1.69×10^{-5}	1.26×10^{-11}	NA[b]
JNA3	3.96×10^5	1.26×10^{-5}	3.20×10^{-11}	NA
JNA10	4.40×10^5	1.20×10^{-6}	2.70×10^{-12}	$<6.48 \times 10^{-12}$
JNA11	5.77×10^5	9.66×10^{-7}	1.67×10^{-12}	$<4.94 \times 10^{-12}$
JNA8	3.43×10^5	1.47×10^{-6}	4.27×10^{-12}	$<2.77 \times 10^{-12}$
JNA14	7.67×10^5	7.96×10^{-7}	1.04×10^{-12}	$<3.10 \times 10^{-12}$

[a] K_D calculated was calculated using the k_d limit and the k_a measured for those VHHs that did not dissociate from ricin within the k_d limit. In several instances little to no VHH dissociation was detected over a 6-h time course, suggesting that the dissociation rate constants were slower than 2×10^{-6} s^{-1} (37). It was therefore not possible to generate a true K_D value. Instead, the K_D was calculated based on the so-called 5% rule that compensates for the limitations of SPR (38). Actual SPR sensorgrams are provided in supplemental Fig. S2.

[b] NA, not applicable.

which is ~10-fold more potent than previously described VHH heterodimers (12) (Table 3 and Fig. 3*A*). JNA8 also had an IC_{50} of 0.1 nM, which was surprising considering that the antibody consists of a weak and a non-neutralizing VHH (Table 3 and Fig. 3*A*).

Based on their *in vitro* profiles, we expected that JNA10, JNA11, and JNA8 would prove effective at neutralizing ricin toxin *in vivo*. To test this, JNA10, JNA11, and JNA8 were each mixed with $10 \times LD_{50}$ of ricin at an 8:1 VHH:toxin molar ratio and administered to mice by intraperitoneal injection. Mice treated with JNA10 (5/5) or JNA11 (5/5) survived the ricin challenge, whereas the group of mice administered JNA8 were only partially (1/5) protected (Fig. 1*C*). These data demonstrate that JNA8 is qualitatively different from JNA10 and JNA11 in the mouse model, even though the three antibodies are indistinguishable from each other in terms of EC_{50} and IC_{50} activities *in vitro*.

VHH Homodimers Demonstrate Potent Toxin-neutralizing Activity in Vitro but Not in Vivo—We next wished to examine the potential of VHH homodimers to neutralize ricin *in vitro* and *in vivo*, with the expectation that monospecific, bivalent antibodies would be highly effective at inactivating ricin toxin. We engineered VHH homodimers JNA6, JNA2, and JNA3 consisting of the strongly toxin-neutralizing monomeric VHHs, RTB-B7, RTA-D10 and RTA-E5, respectively (Tables 2 and 3). We also generated JNA14, a "pseudo"-ho-

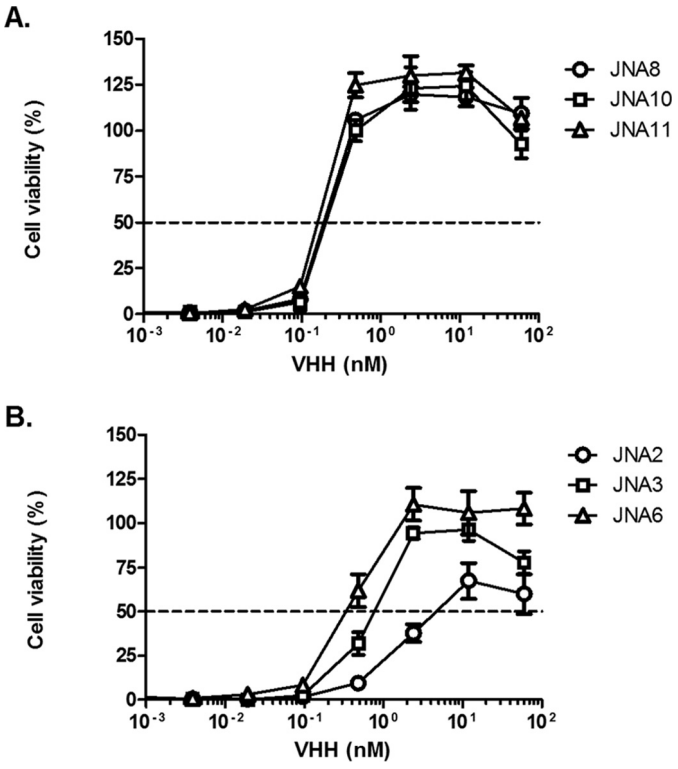

FIGURE 3. ***In vitro* neutralization of ricin toxin by VHH heterodimers and homodimers.** Ricin was mixed with serial dilutions of VHH heterodimers (*A*) JNA8, JNA10, or JNA11 or (*B*) homodimers JNA2, JNA3, or JNA6 and then applied to Vero cells, as described under "Experimental Procedures." Cell viability was measured 48 h later. The results represent a representative experiment done in triplicate with each data point indicating mean ± S.D. Each agent was tested at least twice.

modimer consisting of two different VHHs (RTA-E5 and RTA-D10) that recognize overlapping but distinct structural epitopes on RTA (14).

The specificity of the VHH homodimers for RTA or RTB was demonstrated using ELISA-based soluble competition assays (Fig. 4). As expected, soluble RTA (but not RTB) inhibited the binding of JNA2, JNA3 (Fig. 4, *E, F, H,* and *I*), and JNA14 (data not shown) to plate-bound ricin, whereas soluble RTB (but not RTA) inhibited JNA6 (Fig. 4, *B* and *C*). The actual (or estimated) dissociation constants (K_D) of the VHH homodimers for ricin were determined by SPR and ranged from 1×10^{-11} to 1×10^{-12} M (Table 4).

In the Vero cell cytotoxicity assay, we found that the VHH homodimers were 2.5–12-fold more potent at neutralizing ricin *in vitro* as compared with their respective monomeric constituents, (Tables 2 and 3; Fig. 3*B*). It is interesting to note, however, that the IC_{50} values associated with JNA2 and JNA3 were considerably different (10 *versus* 1 nM) from each other, even though the two antibodies' dissociation constants for ricin were virtually identical (1.26 *versus* 3.20×10^{-11}). This observation demonstrates that there is no clear correlation between antibody affinity and toxin-neutralizing activity.

To evaluate the capacity of VHH homodimers to neutralize ricin *in vivo*, JNA6, JNA2, JNA3, and JNA14 were mixed with ricin at an 8:1 VHH:toxin molar ratio and administered to mice by intraperitoneal injection. We found that none of the VHH homodimers were able to fully protect mice against ricin challenge, even though they did significantly extend the time to death (Fig. 1*D*). Thus, despite their improved avidities for ricin and potent *in vitro* toxin-neutralizing activity, none of the VHH homodimers were able to fully neutralize ricin *in vivo*.

VHH Heterodimers Promote the Formation of Ricin Toxin Aggregates in Solution—We previously reported that VHH heterodimer JJX12 promotes the aggregation of ricin toxin in solution, as evidenced by the formation of high molecular weight species by AUC (11). To examine whether antibody-induced aggregation is a general property associated with VHH heterodimers (particularly those associated with toxin-neutralizing activity *in vivo*), we subjected our new collection of VHH hetero- and homodimers to AUC analysis, in the absence and presence of ricin.

As reported previously, the sedimentation coefficient for ricin was determined to be 4.6S (Fig. 5*A*) (11, 28). The VHH hetero- (JNA10, JNA11, and JNA8) and homo- (JNA2, JNA3, JNA6, and JNA14) dimers had sedimentation coefficients ranging between 2.0S and 3.0S (Fig. 5, *A-F*, and data not shown). In two instances, JNA6 and JNA11, also had minor (7–15%) distributions present at 1.7–1.8S, which may correspond to antibody breakdown products in the preparations. SECMALS results showed no detectable signal that corresponded to the lower molecular weight breakdown product seen with AUC. When the antibodies were mixed with an equimolar ratio of ricin and then subjected to AUC we observed distinct distribution profiles (Fig. 5).

The VHH homodimer-ricin complexes, including the pseudo-heterodimer JNA14, revealed two major distributions with sedimentation coefficients corresponding to 4.9–5.5S and 7.3-7.5S (Fig. 5, *A–C*). We interpret these distributions as corresponding to 1:1 and 1:2 VHH-toxin complexes, respectively. In contrast, the VHH heterodimers, JNA10 and JNA11, each displayed distinct distributions between 8.3 and 8.7S and JNA11 had a long distribution tail with a sedimentation coefficient ≥11.7S (Fig. 5, *E* and *F*). We interpret the 8.3–8.7S distributions as corresponding to a 2:2 VHH:toxin ratio and the sedimentation coefficients ≥11.7S as being heterogeneous mixture of VHH:ricin oligomers. In this respect, the ricin: JNA10 and ricin:JNA11 distribution profiles are virtually identical to what we observed previously for JJX12 (11), JJX3, and JJX21 (data not shown). The ricin-JNA8 VHH heterodimer mixture, on the other hand, displayed a single distribution profile at 5.6S and no evidence of higher molecular weight species (Fig. 5*D*).

Inhibition of Ricin Binding to Cell Surfaces by VHH Homodimers and Heterodimers—We hypothesized that aggregation of ricin toxin by heterodimeric VHH-based antibodies JJX21, JNA10, and JNA11 would affect toxin attachment to cell surfaces. To test this hypothesis, FITC-labeled ricin was mixed with VHH heterodimers and homodimers and applied to THP-1 cells in solution. Adherence of ricin to cell surfaces was determined using flow cytometry. The three VHH heterodimers capable of neutralizing ricin *in vivo*, namely JJX21, JNA10, and JNA11 reduced ricin binding to THP-1 cells by >74% (Fig. 6). The other heterodimer JNA8 and VHH homodimers also interfered with toxin attachment, but to a

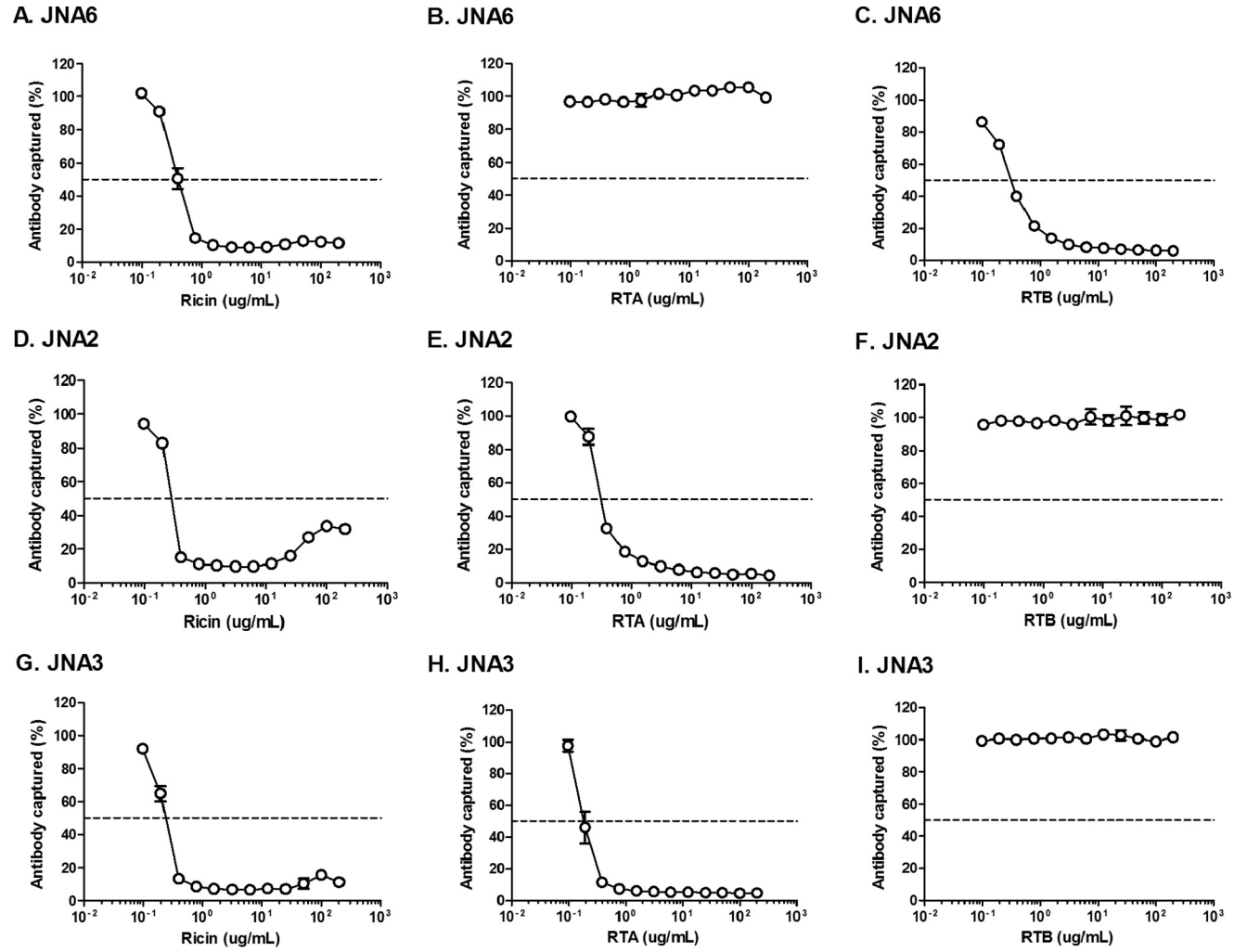

FIGURE 4. **Recognition of soluble ricin and ricin subunits by VHH homodimers.** ELISA plates were coated with ricin and then probed with VHH homodimers JNA6 (*A–C*), JNA2 (*D–F*), or JNA3 (*G–I*) in the presence of 2-fold serial dilutions of soluble ricin (*left panels*), RTA (*middle panels*), or RTB (*right panels*). The percent of antibody bound to the plate is indicated on the *y* axis. The results represent a single representative experiment done in triplicate with each data point indicating mean ± S.D. In most instances error bars are masked by symbols and therefore not visible.

lesser degree than JJX21, JNA10, and JNA11. These results are suggestive of a possible connection between the ability of an antibody to promote ricin aggregation in solution, interfering with attachment to cell surfaces, and neutralizing ricin *in vivo*.

Discussion

VHH-based neutralizing agents consisting of two or more different VHHs covalently linked to each other via a peptide spacer have proven to be extremely effective in mouse (and in one case piglet) models at inactivating an array of different plant- and microbe-derived protein toxins, including botulinum neurotoxin (6), *C. difficile* toxins TcdA and TcdB (7–9), Shiga toxins (10, 29), ricin (11, 12), and anthrax toxin (13). However, with the exception of anthrax toxin, the mechanisms by which these VNAs function *in vitro* and *in vivo* remains poorly understood.

For example, we recently reported that VHH RTB-B7 binds ricin with high affinity and has extremely potent *in vitro* TNA but does not passively protect mice against a ricin challenge (11). However, linking RTB-B7 to any of three different RTA-specific VHHs (RTA-D10, RTA-E5, or RTA-F5) resulted in VHH heterodimers able to neutralize ricin in a mouse model at antibody:toxin molar ratios as low as 4:1 (12). We have now shown that one of these heterodimers, JJX21 (RTA-E5 linked to RTB-B7), has therapeutic potential in that it was able to protect mice from ricin when administered to animals 2 h after toxin exposure. In this regard, JJX21 was as effective as antibody PB10, a well characterized toxin-neutralizing murine mAb that is being considered for advanced development studies, alone or as part of an anti-toxin mixture, in non-human primates (30, 31).

In an effort to better understand the specific attributes of heterodimers that are important in neutralizing ricin *in vivo*, we created three "new" VHH heterodimers, JNA10, JNA11, and JNA8. JNA10 and JNA11 each consisted of a discordant pair of VHH monomers (*i.e.* one with strong *in vitro* toxin-neutralizing activity and one with weak or undetectable toxin-neutralizing activity), whereas JNA8, was the result of partnering two non/poorly neutralizing VHHs. We expected that JNA10, JNA11, and JNA8 would be less effective at neutralizing ricin than JJX21, for example, which is made up of two VHH monomers each with potent toxin-neutralizing activities (12). Surprisingly, in the Vero cell cytotoxicity assay, the three new VHH het-

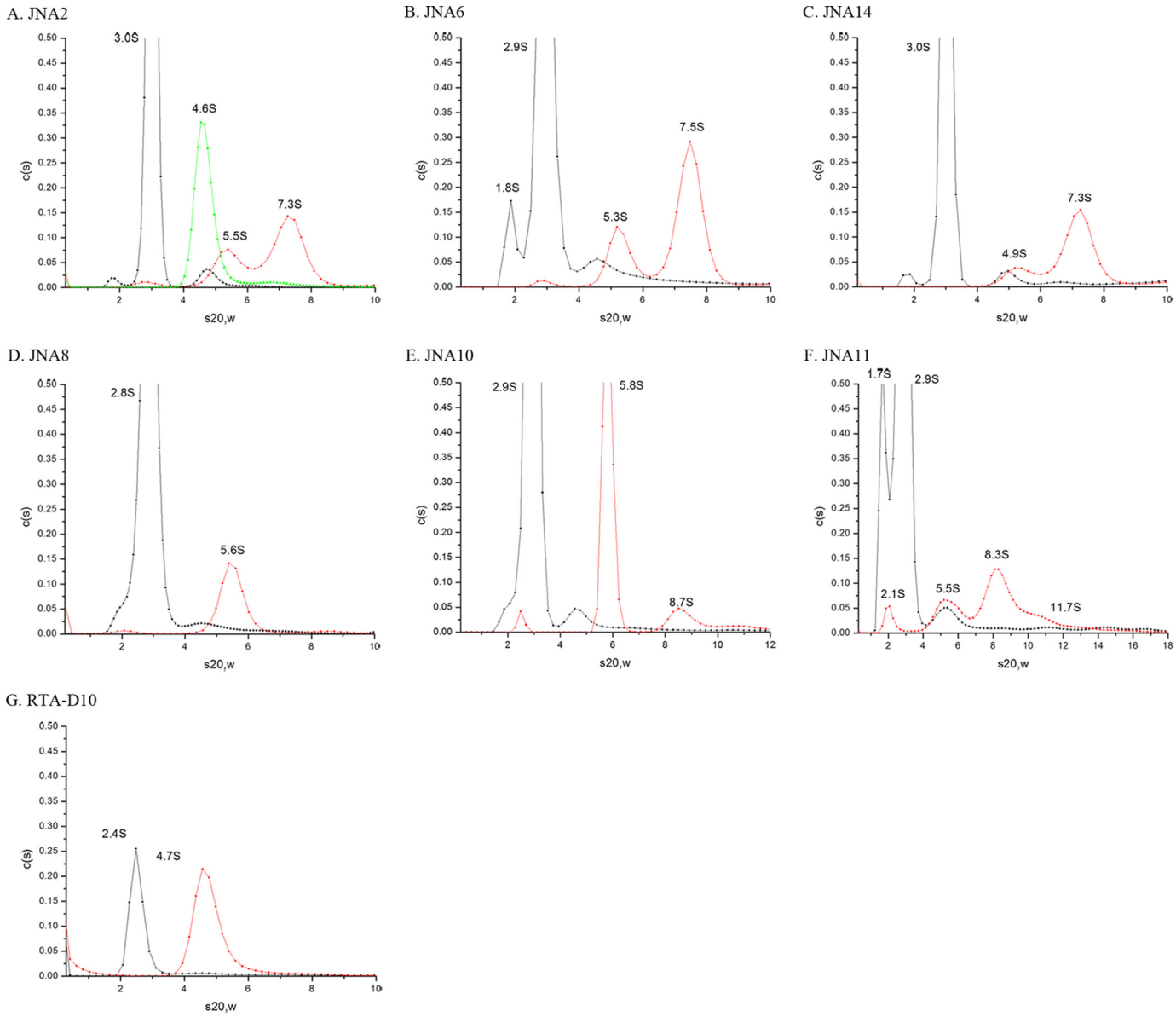

FIGURE 5. **Sedimentation coefficients for ricin and ricin-VHH complexes.** Ricin (*green*), VHH constructs (*black*), or ricin-VHH complexes (*red*) were subject to AUC, as described under "Experimental Procedures." Each *panel* corresponds to a single VHH construct, as indicated in the label. The ricin-VHH mixtures were incubated at room temperature for 1 h before being then subjected to AUC (20 °C). For convenience, the corrected sedimentation coefficients ($s_{20,w}$) are denoted *above* each sedimentation distribution in each plot. The AUC profiles are qualitative in nature and the values associated with the individual *x*- and *y*-axes are adjusted to maximize the visible distributions. VHH homodimers JNA2 and JNA6 are shown in *panels A* and *B,* pseudo-homodimer in *panel C*, VHH heterodimers in *panels D–F*, and a representative VHH monomer in *panel G*.

erodimers (JNA10, JNA11, and JNA8) were 10-fold more potent than JJX21. Thus, the *in vitro* neutralizing activity of VHH heterodimers is not simply the sum of its monomeric constituents, but a consequence possibly related to epitope specificity and/or aggregation potential, as discussed below.

Despite their similarities, JNA10 and JNA11 differed from JNA8 in several important respects. First, JNA10 and JNA11 were able to fully neutralize ricin in the mouse model at an 8:1 VHH:toxin molar ratio, whereas JNA8 afforded only partial protection. Further studies will be necessary to determine whether full protection can be achieved with higher amounts of JNA8. Second, AUC analysis revealed that JNA10 and JNA11 promoted the formation of higher order toxin-antibody complexes ("aggregates") in solution, an observation consistent with the bispecific (anti-RTA and anti-RTB) nature of these two antibodies. Theoretically, JNA10 and JNA11 promote toxin-antibody cross-linking by bridging RTA on one toxin molecule with RTB on a second toxin molecule.

However, AUC analysis indicated that JNA8 did not promote the formation of toxin-antibody aggregates even through the bispecificity of JNA8 for RTA and RTB was demonstrated experimentally. Indeed, the RTA-specific monomer (RTA-F6) of JNA8 is the same as JNA10, and its RTB-specific monomer (RTB-D12) is the same as JNA11 (see Table 3). The failure of JNA8 to cross-link ricin could be related to epitope occlusion of its constitute monomers, RTA-F6 and RTB-D12. For example, RTA-F6 is postulated

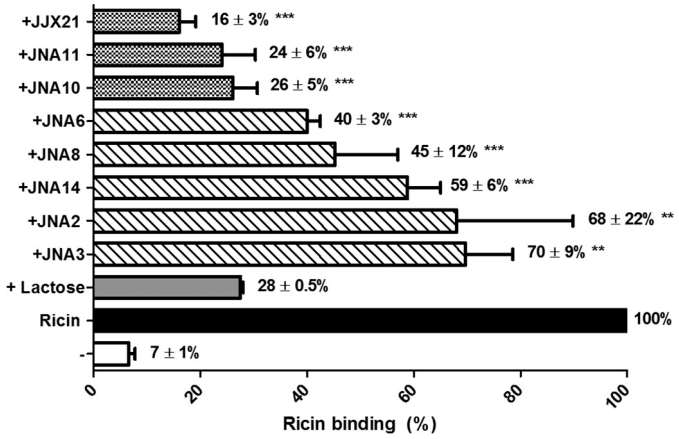

FIGURE 6. **Inhibition of ricin binding to cell surfaces by heterodimeric and homdimeric VHHs.** VHH heterodimers and homodimers were mixed with FITC-labeled ricin prior to being applied to THP-1 cells in solution and then subjected to flow cytometry, as described under "Experimental Procedures." The percent binding was normalized to ricin only treated cells (*solid black bar*). Lactose was used as a known inhibitor of ricin attachment (*gray bar*). Experiments were repeated three independent times and the bar graphs represent each treatment mean ± S.D., values are shown by each corresponding treatment. One-way analysis of variance was used to compare the ricin control to each antibody treatment (**, $p < 0.01$; ***, $p < 0.001$).

to recognize an epitope on RTA at the interface between RTA and RTB (12). If RTB-D12 were to bind an epitope on RTB near that same interface, the two arms of JNA8 would be expected to clash. We are using x-ray crystallography and hydrogen deuterium exchange approaches to delineate the epitopes recognized by RTA-F6 and RTB-D12.

All five VHH heterodimers (JNA10, JNA11, JJX21, JJX3, and JJX12) that are capable of fully neutralizing ricin toxin in the mouse model have now been shown by AUC to promote the formation ricin toxin aggregates in solution (Fig. 5 and data not shown) (11). At this point the relationship between the two readouts (protection and aggregation) is unclear, but the binding studies presented in Fig. 6 may offer a clue. We postulate that aggregation of ricin may not only impede toxin attachment to cell surfaces (as shown in Fig. 6), but may also interfere with retrograde trafficking should the complexes gain access to cellular receptors. We have found that the most potent toxin-neutralizing murine mAbs interfere with ricin transport from the plasma membrane to the trans-Golgi network (32). Preliminary studies using live cell imaging suggest that JJX21 forms toxin-antibody complexes on the surfaces of lung epithelial cells and affects movement of the toxin to the trans-Golgi network cell.[4]

A role for antibody-mediated aggregation in immunity is not a new concept (33, 34), although it is experiencing a resurgence of sorts. For example, Chow *et al.* (35) recently reported that combinations of neutralizing and toxin-enhancing murine mAbs at certain distinct stoichiometries were synergistic at neutralizing anthrax toxin in mice. The same mAb mixtures promoted the formation of higher order toxin-antibody complexes *in vitro*, underscoring the possible importance of toxin aggregation in antibody-mediated protection *in vivo* (35). More recently Galimidi *et al.* (36) demonstrated that cross-linking of the HIV-1 trimeric envelope glycoprotein by homo- and hetero-dimeric Fabs resulted in enhanced *in vitro* neutralizing activity.

As part of this study we also investigated for the first time the potential of VHH homodimers to neutralize a protein toxin *in vitro* and *in vivo*. The results were somewhat unexpected in that none of the three VHH homodimers, two directed against RTA (JNA2 and JNA3) and one against RTB (JNA6) proved capable of fully neutralizing ricin in the mouse model, although they clearly had an effect on ricin based on their ability to extend the mean survival time of an animal as compared with mice that received only toxin. The failure of the RTB-B7 homodimer (JNA6) to afford full protection was particularly surprising given its affinity for ricin and its IC_{50} in the Vero cell cytotoxicity assay were equivalent to those of VHH heterodimers that did neutralize ricin in the mouse. These data demonstrate clearly that avidity alone cannot explain the *in vivo* potency of heterodimeric VHHs like JJX21, JNA10, and JNA11 and lend support to the model that other functional attributes like aggregation may in fact be critical in incapacitating ricin in the context of a mammalian system.

Author Contributions—C. H. conducted the experiments and wrote and edited subsequent drafts of the manuscript. J. M. T. was responsible for producing the recombinant VHH antibodies used in the studies. C. B. S. designed the recombinant antibodies and supervised their production by J. M. T. C. B. S. defined the overall scope of the study. C. B. S. provided ongoing technical assistance throughout the study and edited the manuscript. N. J. M. was responsible for oversight all the experiments conducted at the Wadsworth Center. N. J. M. was responsible for final editing and submission of the manuscript.

Acknowledgments—We thank Drs. Janice Pata, Mike Rudolph, and David Vance for valuable feedback and technical advice. We are most grateful to Leslie Eisele and Renjie Song of the Wadsworth Center's Biochemistry and Immunology Core facility for assistance with AUC and flow cytometry. We also acknowledge Dr. Gary Ross (Bio-Rad) for technical assistance with SPR.

[4] C. Herrera, R. Cole, and N. Mantis, unpublished results.

References

1. Froude, J. W., 2nd, Stiles, B., Pelat, T., and Thullier, P. (2011) Antibodies for biodefense. *MAbs* **3,** 517–527
2. Mantis, N. J., Morici, L. A., and Roy, C. J. (2012) Mucosal vaccines for biodefense. *Curr. Top. Microbiol. Immunol.* **354,** 181–195
3. Reisler, R. B., and Smith, L. A. (2012) The need for continued development of ricin countermeasures. *Adv. Prev. Med.* **2012,** 149737
4. Wolfe, D. N., Florence, W., and Bryant, P. (2013) Current biodefense vaccine programs and challenges. *Hum. Vaccin. Immunother.* **9,** 1591–1597
5. Muyldermans, S. (2013) Nanobodies: natural single-domain antibodies. *Annu. Rev. Biochem.* **82,** 775–797
6. Mukherjee, J., Dmitriev, I., Debatis, M., Tremblay, J. M., Beamer, G., Kashentseva, E. A., Curiel, D. T., and Shoemaker, C. B. (2014) Prolonged prophylactic protection from botulism with a single adenovirus treatment promoting serum expression of a VHH-based antitoxin protein. *PLoS ONE* **9,** e106422
7. Murase, T., Eugenio, L., Schorr, M., Hussack, G., Tanha, J., Kitova, E. N., Klassen, J. S., and Ng, K. K. (2014) Structural basis for antibody recognition in the receptor-binding domains of toxins A and B from *Clostridium difficile*. *J. Biol. Chem.* **289,** 2331–2343

8. Unger, M., Eichhoff, A. M., Schumacher, L., Strysio, M., Menzel, S., Schwan, C., Alzogaray, V., Zylberman, V., Seman, M., Brandner, J., Rohde, H., Zhu, K., Haag, F., Mittrücker, H. W., Goldbaum, F., Aktories, K., and Koch-Nolte, F. (2015) Selection of nanobodies that block the enzymatic and cytotoxic activities of the binary *Clostridium difficile* toxin CDT. *Sci. Rep.* **5,** 7850
9. Yang, Z., Schmidt, D., Liu, W., Li, S., Shi, L., Sheng, J., Chen, K., Yu, H., Tremblay, J. M., Chen, X., Piepenbrink, K. H., Sundberg, E. J., Kelly, C. P., Bai, G., Shoemaker, C. B., and Feng, H. (2014) A novel multivalent, single-domain antibody targeting TcdA and TcdB prevents fulminant Clostridium difficile infection in mice. *J. Infect. Dis.* **210,** 964–972
10. Tremblay, J. M., Mukherjee, J., Leysath, C. E., Debatis, M., Ofori, K., Baldwin, K., Boucher, C., Peters, R., Beamer, G., Sheoran, A., Bedenice, D., Tzipori, S., and Shoemaker, C. B. (2013) A single VHH-based toxin-neutralizing agent and an effector antibody protect mice against challenge with Shiga toxins 1 and 2. *Infect. Immun.* **81,** 4592–4603
11. Herrera, C., Vance, D. J., Eisele, L. E., Shoemaker, C. B., and Mantis, N. J. (2014) Differential neutralizing activities of a single domain camelid antibody (VHH) specific for ricin toxin's binding subunit (RTB). *PLoS ONE* **9,** e99788
12. Vance, D. J., Tremblay, J. M., Mantis, N. J., and Shoemaker, C. B. (2013) Stepwise engineering of heterodimeric single domain camelid VHH antibodies that passively protect mice from ricin toxin. *J. Biol. Chem.* **288,** 36538–36547
13. Moayeri, M., Leysath, C. E., Tremblay, J. M., Vrentas, C., Crown, D., Leppla, S. H., and Shoemaker, C. B. (2015) A heterodimer of a VHH (variable domains of camelid heavy chain-only) antibody that inhibits anthrax toxin cell binding linked to a VHH antibody that blocks oligomer formation is highly protective in an anthrax spore challenge model. *J. Biol. Chem.* **290,** 6584–6595
14. Rudolph, M. J., Vance, D. J., Cheung, J., Franklin, M. C., Burshteyn, F., Cassidy, M. S., Gary, E. N., Herrera, C., Shoemaker, C. B., and Mantis, N. J. (2014) Crystal structures of ricin toxin's enzymatic subunit (RTA) in complex with neutralizing and non-neutralizing single-chain antibodies. *J. Mol. Biol.* **426,** 3057–3068
15. Chen, C., Przedpelski, A., Tepp, W. H., Pellett, S., Johnson, E. A., and Barbieri, J. T. (2015) Heat-labile enterotoxin IIa, a platform to deliver heterologous proteins into neurons. *MBio* **6,** e00734
16. Vance, D. J., Rong, Y., Brey, R. N., 3rd, and Mantis, N. J. (2015) Combination of two candidate subunit vaccine antigens elicits protective immunity to ricin and anthrax toxin in mice. *Vaccine* **33,** 417–421
17. Audi, J., Belson, M., Patel, M., Schier, J., and Osterloh, J. (2005) Ricin poisoning: a comprehensive review. *JAMA* **294,** 2342–2351
18. Endo, Y., Mitsui, K., Motizuki, M., and Tsurugi, K. (1987) The mechanism of action of ricin and related toxins on eukaryotic ribosomes. *J. Biol. Chem.* **262,** 5908–5912
19. Endo, Y., and Tsurugi, K. (1987) RNA *N*-glycosidase activity of ricin A-chain: mechanism of action of the toxic lectin ricin on eukaryotic ribosomes. *J. Biol. Chem.* **262,** 8128–8130
20. Rutenber, E., Ready, M., and Robertus, J. D. (1987) Structure and evolution of ricin B chain. *Nature* **326,** 624–626
21. Sandvig, K., Olsnes, S., and Pihl, A. (1976) Kinetics of binding of the toxic lectins abrin and ricin to surface receptors of human cells. *J. Biol. Chem.* **251,** 3977–3984
22. Sandvig, K., Skotland, T., van Deurs, B., and Klokk, T. I. (2013) Retrograde transport of protein toxins through the Golgi apparatus. *Histochem. Cell Biol.* **140,** 317–326
23. Spooner, R. A., and Lord, J. M. (2012) How ricin and Shiga toxin reach the cytosol of target cells: retrotranslocation from the endoplasmic reticulum. *Curr. Top. Microbiol. Immunol.* **357,** 19–40
24. Mukherjee, J., Tremblay, J. M., Leysath, C. E., Ofori, K., Baldwin, K., Feng, X., Bedenice, D., Webb, R. P., Wright, P. M., Smith, L. A., Tzipori, S., and Shoemaker, C. B. (2012) A novel strategy for development of recombinant antitoxin therapeutics tested in a mouse botulism model. *PLoS ONE* **7,** e29941
25. Yermakova, A., and Mantis, N. J. (2011) Protective immunity to ricin toxin conferred by antibodies against the toxin's binding subunit (RTB). *Vaccine* **29,** 7925–7935
26. Schuck, P., Perugini, M. A., Gonzales, N. R., Howlett, G. J., and Schubert, D. (2002) Size-distribution analysis of proteins by analytical ultracentrifugation: strategies and application to model systems. *Biophys. J.* **82,** 1096–1111
27. O'Hara, J. M., Whaley, K., Pauly, M., Zeitlin, L., and Mantis, N. J. (2012) Plant-based expression of a partially humanized neutralizing monoclonal IgG directed against an immunodominant epitope on the ricin toxin A subunit. *Vaccine* **30,** 1239–1243
28. Frénoy, J. P. (1986) Effect of physical environment on the conformation of ricin: influence of low pH. *Biochem. J.* **240,** 221–226
29. Sheoran, A. S., Dmitriev, I. P., Kashentseva, E. A., Cohen, O., Mukherjee, J., Debatis, M., Shearer, J., Tremblay, J. M., Beamer, G., Curiel, D. T., Shoemaker, C. B., and Tzipori, S. (2015) Adenovirus vector expressing Stx1/Stx2-neutralizing agent protects piglets infected with *Escherichia coli* O157:H7 against fatal systemic intoxication. *Infect. Immun.* **83,** 286–291
30. Sully, E. K., Whaley, K. J., Bohorova, N., Bohorov, O., Goodman, C., Kim do, H., Pauly, M. H., Velasco, J., Hiatt, E., Morton, J., Swope, K., Roy, C. J., Zeitlin, L., and Mantis, N. J. (2014) Chimeric plantibody passively protects mice against aerosolized ricin challenge. *Clin. Vaccine Immunol.* **21,** 777–782
31. Sully, E. K., Whaley, K., Bohorova, N., Bohorov, O., Goodman, C., Kim, D., Pauly, M., Velasco, J., Holtsberg, F. W., Stavale, E., Aman, M. J., Tangudu, C., Uzal, F. A., Mantis, N. J., and Zeitlin, L. (2014) A tripartite cocktail of chimeric monoclonal antibodies passively protects mice against ricin, staphylococcal enterotoxin B and *Clostridium perfringens* ϵ toxin. *Toxicon* **92,** 36–41
32. Yermakova, A., Klokk, T. I., Cole, R., Sandvig, K., and Mantis, N. J. (2014) Antibody-mediated inhibition of ricin toxin retrograde transport. *MBio* **5,** e00995
33. Brioen, P., Dekegel, D., and Boeyé, A. (1983) Neutralization of poliovirus by antibody-mediated polymerization. *Virology* **127,** 463–468
34. Thomas, A. A., Vrijsen, R., and Boeyé, A. (1986) Relationship between poliovirus neutralization and aggregation. *J. Virol.* **59,** 479–485
35. Chow, S. K., Smith, C., MacCarthy, T., Pohl, M. A., Bergman, A., and Casadevall, A. (2013) Disease-enhancing antibodies improve the efficacy of bacterial toxin-neutralizing antibodies. *Cell Host Microbe* **13,** 417–428
36. Galimidi, R. P., Klein, J. S., Politzer, M. S., Bai, S., Seaman, M. S., Nussenzweig, M. C., West, A. P., Jr., and Bjorkman, P. J. (2015) Intra-spike crosslinking overcomes antibody evasion by HIV-1. *Cell* **160,** 433–446
37. Abdiche, Y. N., Malashock, D. S., and Pons, J. (2008) Probing the binding mechanism and affinity of tanezumab, a recombinant humanized anti-NGF monoclonal antibody, using a repertoire of biosensors. *Protein Sci.* **17,** 1326–1335
38. Katsamba, P. S., Navratilova, I., Calderon-Cacia, M., Fan, L., Thornton, K., Zhu, M., Bos, T. V., Forte, C., Friend, D., Laird-Offringa, I., Tavares, G., Whatley, J., Shi, E., Widom, A., Lindquist, K. C., Klakamp, S., Drake, A., Bohmann, D., Roell, M., Rose, L., Dorocke, J., Roth, B., Luginbühl, B., and Myszka, D. G. (2006) Kinetic analysis of a high-affinity antibody/antigen interaction performed by multiple Biacore users. *Anal. Biochem.* **352,** 208–221